The Journal of Experimental Biology 215, 508-517

doi:10.1242/jeb.060004

RESEARCH ARTICLE

Independence of net water flux from paracellular permeability in the intestine of *Fundulus heteroclitus*, a euryhaline teleost

Chris M. Wood[1,2,*] and Martin Grosell[1]

[1]Rosenstiel School of Marine and Atmospheric Sciences, University of Miami, Miami, FL 33149, USA and [2]Department of Biology, McMaster University, 1280 Main Street West, Hamilton, ON, Canada, L8S 4K1

*Author for correspondence (woodcm@mcmaster.ca)

Accepted 2 November 2011

SUMMARY

Paracellular permeability and absorptive water flux across the intestine of the euryhaline killifish were investigated using *in vitro* gut sac preparations from seawater- and freshwater-acclimated animals. The permeability of polyethylene glycol (PEG), a well-established paracellular probe, was measured using trace amounts of radiolabelled oligomers of three different molecular sizes (PEG-400, PEG-900 and PEG-4000) at various times after satiation feeding. All three PEG molecules were absorbed, with permeability declining as a linear function of increasing hydrodynamic radius. Response patterns were similar in seawater and freshwater preparations, though water absorption and PEG-900 permeability were greater in the latter. Despite up to 4-fold variations in absorptive water flux associated with feeding and fasting (highest at 1–3 h, lowest at 12–24 h and intermediate at 1–2 weeks post-feeding), there were no changes in PEG permeability for any size oligomer. When PEG permeability was measured in the opposite direction (i.e. serosal to mucosal) from net water flux, it was again unchanged. $HgCl_2$ (10^{-3} mol l^{-1}), a putative blocker of aquaporins, eliminated absorptive water flux yet increased PEG-4000 permeability by 6- to 8-fold in both freshwater and seawater preparations. Experimentally raising the serosal osmolality by addition of 300 mmol l^{-1} mannitol increased the absorptive water flux rate 10-fold, but did not alter PEG permeability. Under these conditions, $HgCl_2$ reduced absorptive water flux by 60% and again increased PEG permeability by 6- to 8-fold in both freshwater and seawater preparations. Clearly, there was no influence of solvent drag on PEG movement. The putative paracellular blocker 2,4,6-triaminopyrimidine (TAP, 20 mmol l^{-1}) had no effect on net water flux or PEG permeability. We conclude that PEG and water move by separate pathways; absorptive water transport probably occurs *via* a transcellular route in the intestine of *Fundulus heteroclitus*.

Key words: paracellular permeability, transcellular permeability, feeding, fasting, Cl^- uptake, solvent drag, polyethylene glycol, PEG.

INTRODUCTION

As in most marine teleosts (Grosell, 2006), the intestine of the common killifish *Fundulus heteroclitus* absorbs a fluid that is strongly hypertonic on a net basis (Wood et al., 2010). In recent years, great strides have been made in understanding the ion transport mechanisms that help drive this water absorption (reviewed by Wilson et al., 2002; Wilson and Grosell, 2003; Grosell, 2006; Grosell and Taylor, 2007; Grosell et al., 2009; Grosell, 2011a; Grosell, 2011b). However, there has been little progress on the equally important question of how the water actually moves. Is the net flux by a transcellular route, a paracellular route, or a combination of the two? In this regard, the teleost intestine is not unusual. In a recent review, Hill (Hill, 2008) noted: 'The transport of fluid is one of the fundamental processes in physiology… Despite a voluminous literature, there is no clear idea of how it occurs.'

Our investigation of this problem was stimulated by two observations. Firstly, in the course of a study on the impact of feeding on ion and acid–base transport in the killifish gut (Wood et al., 2010), we found that there were large increases in ion and water absorption immediately after feeding, which had attenuated by 12–24 h. Secondly, and somewhat surprisingly, these changes tended to be larger in the intestines of freshwater-acclimated killifish. We therefore exploited these natural differences in fluid absorption rates, associated with feeding and salinity, to see whether there were corresponding differences in paracellular permeability, using three polyethylene glycol (PEG) oligomers of increasing size (PEG-400, PEG-900 and PEG-4000). PEG is well established as a paracellular marker in intestinal tissues (Pappenheimer and Reiss, 1987; Watson et al., 2001). We reasoned that if some of the increased absorptive water flux was paracellular, we would expect to find a greater PEG permeability, especially if there was a convective solvent drag component to water movement (Whittembury et al., 1980; Pappenheimer and Reiss, 1987; Ma et al., 1991). A differential response with the different size oligomers of PEG might provide information on the size of the particular paracellular channels involved (He et al., 1998; Watson et al., 2001). We followed up these experiments by measuring PEG permeability in the serosal to mucosal direction, i.e. in the opposite direction from net water flux. We also examined PEG permeability under conditions of osmotic clamping, where the net mucosal to serosal water flux was increased 10-fold. The influence of $HgCl_2$, a general inhibitor of aquaporins in the transcellular pathway (Cerda and Finn, 2010), was examined on water flux and PEG permeability under isosmotic conditions, and under osmotic clamping. Finally, we measured PEG permeability and water flux in the presence of a putative blocker of the paracellular pathway, 2,4,6-triaminopyrimidine (TAP) (Rehman et al., 2003).

Our results tell a simple story. There appears to be absolutely no effect of altered net water flux on PEG permeability, regardless of

the size of the PEG molecules. $HgCl_2$ treatment reduces or eliminates absorptive water flux yet greatly increases PEG permeability, whereas TAP has no effect. We conclude that absorptive water transport is very probably by a transcellular route in the intestine of *F. heteroclitus*.

MATERIALS AND METHODS

Experimental animals

Experiments were performed on gut sac preparations from ~340 common killifish of the northern subspecies *Fundulus heteroclitus macrolepidotus* (Walbaum 1792) (3–10 g). The fish were collected by Aquatic Research Organisms (ARO) Ltd (Hampton, NH, USA) by beach-seining of local tidal flats, and then shipped to the University of Miami where they were held for at least 2 months prior to experiments. Acclimation and experimental temperature was 22–24°C. Killifish were kept in large groups (30–50 animals per 50 l tank) in either freshwater or seawater. For freshwater acclimation, salinity was changed gradually over 48 h in several of the tanks, and then the animals were held in flowing freshwater for at least 20 days prior to test. The composition of Miami seawater (37.5 p.p.t.) and freshwater have been reported previously (Wood and Grosell, 2008). Additional fish from the same source were shipped to McMaster University for the pharmacological experiments. At McMaster, they were held in the same water quality (synthetic seawater of the same salinity, or synthetic freshwater duplicating Miami freshwater) as at Miami, but in filtered tanks in which the water was renewed weekly. In both freshwater and seawater, the animals were fed Aqua Max sinking pellets (50% protein) with the following measured ionic composition ($\mu mol\,g^{-1}$): Na^+ 230, Cl^- 170, Ca^{2+} 628, Mg^{2+} 77 and K^+ 326, at a daily ration of ~1.5%. The standard protocol was to keep the fish on the 1.5% daily ration prior to an experiment, then fast them for 48 h, followed by administration of a satiation meal. Test dissections showed that the ingested ration was typically 3–4% of body mass.

The experiments were approved by institutional animal care committees at the University of Miami and McMaster University.

Standard gut sac experiments

In preliminary trials, we found that net water transport and PEG permeability were the same when measured over 1, 2 and 3 h periods, but not thereafter; a standard 2 h period was used in most experiments. Fish were killed for gut sac experiments at 1–3 h post-feeding, 12–24 h post-feeding, and after 7–14 days of fasting in both freshwater and seawater. At each time and at each salinity, flux experiments were performed on 6–9 different preparations for each of three different molecular masses (400, 900, 4000 Da) of radiolabelled PEG ([^{3}H]PEG-400, [^{3}H]PEG-900, [^{14}C]PEG-4000; American Radiochemicals, St Louis, MO, USA). A modified Cortland saline (Wolf, 1963) was used for all gut sac preparations ($mmol\,l^{-1}$): NaCl 144, KCl 5.1, $CaCl_2{\cdot}2H_2O$ 1.4, $MgSO_4{\cdot}7H_2O$ 1.9, $NaHCO_3$ 11.9, Na_2HPO_4 2.9 and glucose 5.5. The osmolality was 303 $mosmol\,kg^{-1}$. The saline was gassed with a 0.3% CO_2 and 99.7% O_2 mixture (i.e. nominal P_{CO2}=2.25 Torr, P_{O2}>700 Torr, where 1 Torr=133 Pa) and the pH was adjusted to 8.12 with small amounts of 1 $mol\,l^{-1}$ HCl. In each gut sac preparation, one of the radiolabelled PEG compounds was placed in the mucosal saline at a concentration of 0.5–1.0 $\mu Ci\,ml^{-1}$, representing a maximum total PEG concentration of 0.5–1.0 $\mu g\,ml^{-1}$.

Methods generally followed those developed earlier (Scott et al., 2006). Fish were lightly anaesthetized in MS-222 (0.1 $g\,l^{-1}$), killed by cephalic concussion, and the intestinal tract dissected out while the fish was kept cold on ice. The killifish is agastric, with the oesophagus entering directly into the anterior intestine through a pylorus-like sphincter. The entire tract from this point back to the anus was removed and formed into a single gut sac preparation. This comprises the anterior, mid and posterior sections corresponding to the first, second and third portions in the diagram of Babkin and Bowie (Babkin and Bowie, 1928); the distal 10% of the tract (corresponding to the point where the posterior intestine joins the rectum) was excluded because it was found to be very fragile. The preparation was flushed thoroughly with ice-cold saline to clear out food and chyme. The distal end of the intestine was then tied off and a heat-flared catheter (PE 90 polyethylene tubing) secured into the other end with 2-0 silk suture. The sac was then filled with radiolabelled saline (typically 200–600 µl depending on fish size), taking care not to trap air bubbles, a sample (100 µl) of the filling saline was taken for analysis of initial mucosal radioactivity ($[PEG_m{*}]_i$), and the catheter was then sealed with a pin. The preparation was blotted on tissue paper in a standardized manner, weighed to 0.1 mg accuracy on an analytical balance, then suspended in a Falcon^{TM} tube containing 11 ml of the same saline (but lacking the radiolabelled PEG). The external saline was continually bubbled with the humidified gas mixture (99.7% O_2, 0.3% CO_2) and a constant temperature of 23°C was maintained by a water bath. After 1 min, a 5 ml sample was taken for recording of initial serosal radioactivity ($[PEG_s{*}]_i$). A 2 h incubation period ensued, during which time the external saline volume was 6 ml. A final 5 ml sample of external saline was taken for recording of final serosal radioactivity ($[PEG_s{*}]_f$). The preparation was blotted and weighed exactly as before for gravimetric determination of fluid transport rate. The contents of the sac were collected for analysis of final mucosal saline radioactivity ($[PEG_s{*}]_m$). The empty sac was then blotted dry and weighed. Subtraction of this mass from the initial and final filled masses yielded the initial (V_i) and final (V_f) mucosal saline volumes, respectively. Finally, the sac was cut open, wetted, stretched to maximum size on graph paper, and the gross area (A) of the exposed epithelial surface determined by tracing its outline onto the paper (Grosell and Jensen, 1999).

All samples for measurement of [^{3}H]PEG or [^{14}C]PEG radioactivity were counted in a total volume of 5 ml saline plus 10 ml of Ecolume fluor (MP Biomedicals, St Louis, MO, USA). Tests showed that quench was constant. Cl^- was measured by coulometric titration (Radiometer-Copenhagen CMT 10, Copenhagen, Denmark).

Net water transport rates ($\mu l\,cm^{-2}\,h^{-1}$) were calculated from the difference between initial (V_i) and final (V_f) mucosal saline volumes, factored by the intestinal surface area (A, cm^2) and time (T, h).

PEG permeability was calculated as:

$$P_{PEG} = \frac{([PEG_s{*}]_f - [PEG_s{*}]_i) \times 6}{0.5([PEG_m{*}]_i + [PEG_m{*}]_f) \times T \times 3600 \times A}\ , \quad (1)$$

where P_{PEG} is in $cm\,s^{-1}$, PEG* radioactivities are in $c.p.m.\,ml^{-1}$, T is in h, A is in cm^2, 6 refers to the external volume in ml and 3600 converts hours to seconds.

The relative PEG flux/water flux ratio was calculated as:

$$\text{Flux ratio} = \frac{([PEG_s{*}]_f - [PEG_s{*}]_i) \times 6}{0.5([PEG_m{*}]_i + [PEG_m{*}]_f) \times (V_i - V_f)}\ . \quad (2)$$

If the flux ratio is 1.0, PEG is moving at the same relative rate as water. If it is greater than 1.0, PEG is moving faster than water, and if it is less than 1.0, PEG is moving at a slower rate than water.

Reverse permeability gut sac experiments

In the standard gut sac experiments, PEG permeability was measured by tracking the flux of PEG radioactivity in the same direction as the absorptive water flux, i.e. from mucosal to serosal compartments. In contrast, in this experiment, PEG permeability was measured by

tracking PEG radioactivity flux from serosal to mucosal compartments, i.e. in the opposite direction from net water flux. Experiments were performed only with ^{3}[H]PEG-400 and ^{14}[C]PEG-4000 (N=6–8 per treatment) on preparations taken at 12–24 h post-feeding from seawater killifish. The preparations were made in the standard fashion, but the radioactive PEG was added at the normal concentration (0.5–1.0 μCi ml^{-1}) to the serosal saline, which had a volume of only 2 ml (otherwise a vast amount of radioactivity would have been used). Simultaneous controls were run where PEG permeability was measured in the standard fashion. Net water flux was calculated in the standard manner, but PEG permeability was calculated from the appearance of radioactivity in the mucosal saline:

$$P_{PEG} = \frac{([PEG_m{*}]_f \times V_f) - ([PEG_m{*}]_i \times V_i)}{0.5([PEG_s{*}]_i + [PEG_s{*}]_f) \times T \times 3600 \times A} \quad . \qquad (3)$$

This approach was used in preference to everted gut sac preparations, as initial trials indicated that this unnatural procedure resulted in damage, manifesting as greatly increased PEG-4000 permeabilities and decreased net water transport rates.

Osmotic clamping gut sac experiments

Preparations were made in the standard fashion, but 300 mmol l^{-1} of mannitol was added to the serosal saline to accelerate the fluid transport rate. This raised the measured serosal osmolality from 303 to 580 mosmol kg^{-1}. Simultaneous controls were run where the serosal osmolality was maintained at 303 mosmol kg^{-1}. Experiments were performed only with ^{3}[H]PEG-400 and ^{14}[C]PEG-4000 (N=6–8 per treatment) on preparations made at 12–24 h post-feeding from seawater killifish, which exhibited the lowest endogenous water absorption rates at this time. As absorptive water flux rates were elevated in the experimental treatment, the incubation period was shortened to 1 h. Net water flux rates and PEG permeabilities (Eqn 1) were calculated as outlined above.

$HgCl_2$ gut sac experiments

Mercuric chloride ($HgCl_2$; Sigma-Aldrich, St Louis, MO, USA) is an effective blocker of most fish aquaporins (Cerda and Finn, 2010), including several recently cloned from *F. heteroclitus* (Tingaud-Sequeira et al., 2009). Tests were performed with $HgCl_2$ concentrations of either 10^{-4} or 10^{-3} mol l^{-1} on preparations made at 12–24 h post-feeding from both seawater killifish and freshwater killifish (i.e. four separate trials, N=7–11 per treatment). Gut sac preparations were made in the standard manner, but were pre-incubated with $HgCl_2$ on the mucosal surface only for 0.5 h before the flux measurement began. $HgCl_2$ remained present in the mucosal saline during the flux measurement. Controls were run simultaneously with the same pre-incubation protocol but without $HgCl_2$. Net water flux rates and PEG permeabilities were calculated as above.

Osmotic clamping plus $HgCl_2$ gut sac experiments

The osmotic clamping and $HgCl_2$ treatments were combined, using a mucosal $HgCl_2$ concentration of 10^{-3} mol l^{-1} and a serosal osmolality of 580 mosmol kg^{-1}, achieved by the addition of 300 mmol l^{-1} mannitol to the serosal saline. The 0.5 h pre-incubation with $HgCl_2$ on the mucosal surface occurred before the serosal osmolality was raised to 580 mosmol kg^{-1}. Experiments were performed on gut sacs made at 12–24 h post-feeding from both seawater killifish and freshwater killifish (i.e. two separate trials, N=6–8 per treatment). Simultaneous controls involved pre-incubation and exposure to high serosal osmolality, but without the addition of mucosal $HgCl_2$. Net water flux rates and PEG permeabilities were calculated as above.

TAP gut sac experiments

The compound TAP (Sigma-Aldrich) is a putative paracellular pathway blocker that has been reported to greatly reduce water absorption in the small intestine of the rat (Rehman et al., 2003). TAP was tested in four separate series (N=6–9 per treatment) for its effects on water absorption and ^{14}[C]PEG-4000 permeability in gut sac preparations from seawater killifish at 1–3 or 12–24 h post-feeding. TAP was added to the mucosal saline at a concentration of 20 mmol l^{-1}, which is effective in rat intestine (Rehman et al., 2003), either with or without 1 h pre-incubation before the flux measurement was started. TAP remained present in the mucosal saline during the flux measurement. Mannitol, at a concentration of 20 mmol l^{-1}, was added to the serosal saline to balance osmotic pressure. Controls with the same concentrations of mannitol on both surfaces were run simultaneously. Net water flux rates and PEG permeabilities were calculated as above.

Statistical analyses

Data are reported as means ± s.e.m. (N=number of gut sac preparations). In a few cases, data were log-transformed so as to pass tests of normality (Shapiro–Wilk) and homogeneity (Bartlett's chi square) prior to further statistical analysis. One-way ANOVA followed by Fisher's LSD test was used for comparison of means within a salinity. Differences between freshwater and seawater animals at specific times or between specific treatments were determined using Student's unpaired t-test. Tests were two-tailed and values were considered significantly different at P<0.05.

RESULTS

Gut PEG permeability and water absorption in seawater killifish with respect to time post-feeding

Permeability to PEG in preparations from seawater fish was essentially independent of time post-feeding, but strongly dependent on the molecular size of the PEG oligomer (Fig. 1A). Permeability fell from about 15–18 ($\times10^{-7}$) cm s^{-1} for PEG-400 to 9–14 ($\times10^{-7}$) cm s^{-1} for PEG-900 and to 1–3 ($\times10^{-7}$) cm s^{-1} for PEG-4000. The only significant effect of time post-feeding was a higher permeability to PEG-4000 in fish that had been fasted for 1–2 weeks.

This pattern was completely different from the pattern in absorptive water flux (Fig. 1B), which was greatest immediately after feeding (8–11 μl cm^{-2} h^{-1}), at a minimum at 12–24 h post-feeding (2–3 μl cm^{-2} h^{-1}), and intermediate in long-term fasted fish (4–5 μl cm^{-2} h^{-1}). Note that net water flux was independent of the size of the PEG molecules, which is to be expected as only trace amounts of radiolabelled PEG were used.

The disconnect of PEG permeability from water absorption was emphasized by calculation of the relative PEG flux to net water flux ratio (Fig. 1C). The ratio exhibited wide divergence from 1.0, being well below 1.0 at all times for PEG-4000, but above 1.0 for PEG-400 and PEG-900 at 12–24 h post-feeding, the time of lowest net water flux (Fig. 1B).

Gut PEG permeability and water absorption in freshwater killifish with respect to time post-feeding

Overall patterns were very similar to those in seawater killifish, with PEG permeability again being independent of time post-feeding but strongly dependent on the size of the PEG molecule (Fig. 2A). PEG permeability tended to be slightly higher in freshwater preparations, but the only significant difference between freshwater and seawater fish was a higher permeability to PEG-4000 in freshwater preparations at 1–3 h post-feeding.

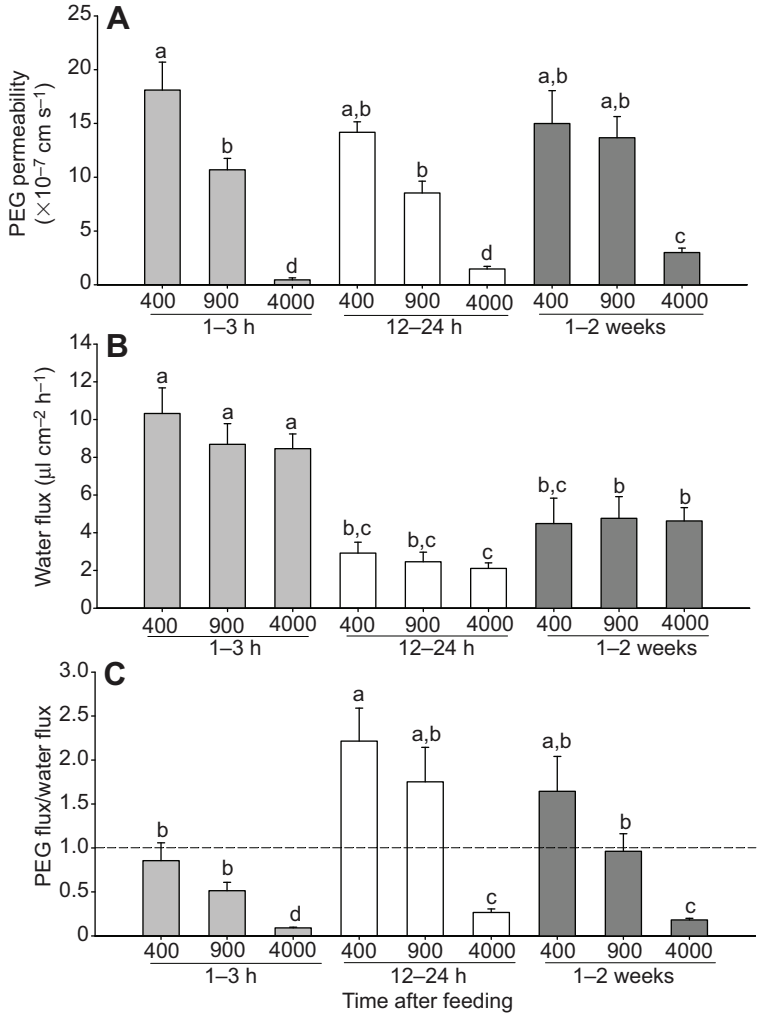

Fig. 1. (A) Permeability of intestinal sac preparations from seawater-acclimated killifish to PEG-400, PEG-900 and PEG-4000 at 0–3 h, 12–24 h and 1–2 weeks after a satiation meal. Permeability was measured in the mucosal to serosal direction. (B) Simultaneously measured absorptive flux of water in the mucosal to serosal direction in these same preparations. (C) The relative PEG flux to net water flux ratio in these same preparations; if the flux ratio is >1.0, PEG is moving faster than water, and if it is <1.0, PEG is moving at a slower rate than water. See Materials and methods for details. Means + 1 s.e.m. (*N*=6–9 per treatment). Within a panel, means sharing the same letter are not significantly different from one another ($P>0.05$).

Again, the pattern in net water flux (Fig. 2B) was completely different from the pattern in PEG permeability. Absorptive water flux tended to be higher in freshwater preparations, differences that were significant in the PEG-4000 treatment at 1–3 h post-feeding, and in all treatments at 12–24 h post-feeding. Absorptive water flux was again not affected by the size of the PEG molecules.

Calculation of the relative PEG flux to water flux ratio (Fig. 2C) again highlighted the lack of correlation between PEG permeability, which was relatively constant, and net water flux, which varied greatly.

Reverse permeability gut sac experiments

In this experiment with seawater preparations at 12–24 h post-feeding, PEG permeability was measured in the serosal to mucosal direction, opposite to the net absorptive flow of water from mucosal to serosal compartments (Fig. 3A). Both PEG-400 permeability and PEG-4000 permeability were unchanged, regardless of whether the PEG flux was in the same direction or the opposite direction to the net water flux.

Osmotic clamping gut sac experiments

When the osmolality of the serosal medium was increased from 303 to 580 mosmol kg^{-1} in seawater preparations at 12–24 h post-feeding, the rate of absorptive water flux was accelerated by about 10-fold (Fig. 4A). This had no effect on the permeability to PEG-400 or PEG-4000 measured in the same direction (Fig. 4B), again highlighting the lack of coupling of PEG and net water flux.

$HgCl_2$ gut sac experiments

The preceding results pointed to a route for absorptive water flux that was different from the paracellular PEG pathway. Aquaporins could offer a transcellular route, so the effect of the aquaporin blocker $HgCl_2$, applied mucosally, was evaluated. As aquaporin expression is reported to differ between freshwater and seawater teleosts (see Discussion), experiments were performed with preparations from both salinities at 12–24 h post-feeding. At 10^{-4} mol l^{-1}, $HgCl_2$ had no effect on absorptive water flux or PEG-4000 permeability in either freshwater or seawater gut sacs (data not shown). However, at 10^{-3} mol l^{-1}, $HgCl_2$ effectively abolished water absorption (Fig. 5A) while increasing PEG-4000 permeability by about 6-fold (Fig. 5B) in both freshwater and seawater preparations, again indicating a complete dissociation between PEG and water flux. While these results might suggest an important role for aquaporins, it should be noted that 10^{-3} mol l^{-1} $HgCl_2$ virtually eliminated absorptive Cl^- flux (freshwater: 297±72 nmol cm^{-2} h^{-1} *N*=8 *versus* 1728±269 nmol cm^{-2} h^{-1} *N*=11; seawater: 25±243 nmol cm^{-2} h^{-1} *N*=7 *versus* 1194±72 nmol cm^{-2} h^{-1} *N*=7). Thus, a major driving force for water absorption was also inhibited.

Osmotic clamping plus $HgCl_2$ gut sac experiments

The goal here was to evaluate the influence of $HgCl_2$ in a situation where an imposed osmotic gradient, rather than Cl^- transport, would be the major driving force for water absorption.

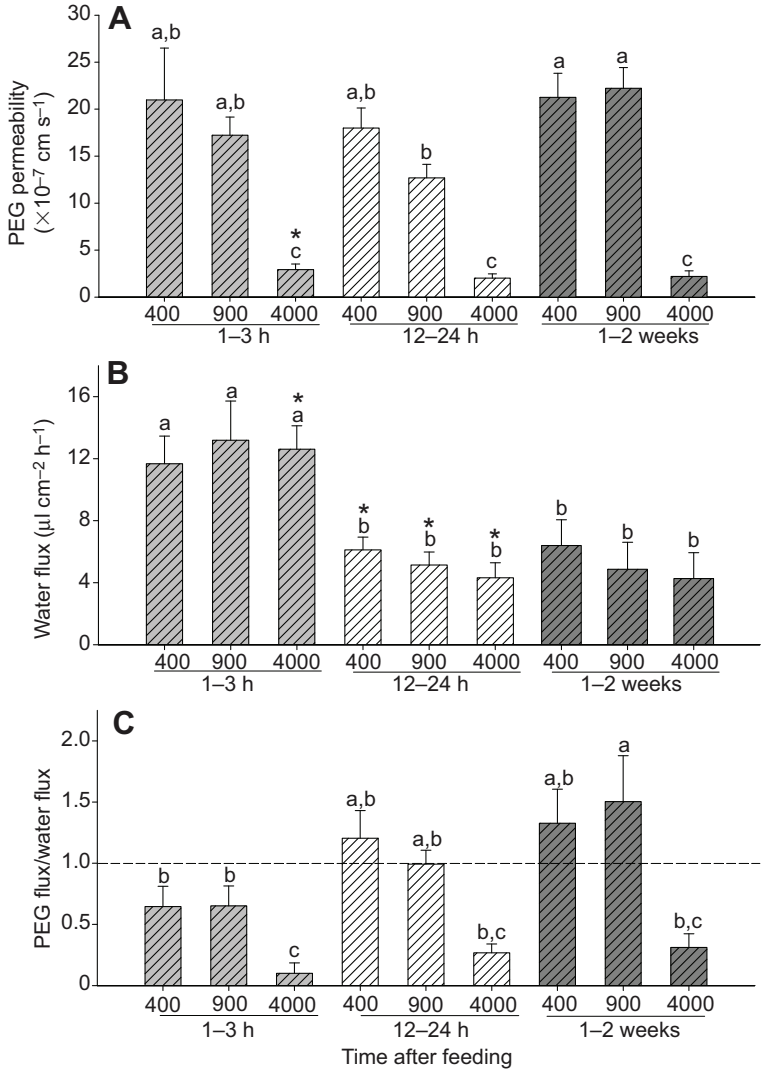

Fig. 2. (A) Permeability of intestinal sac preparations from freshwater-acclimated killifish to PEG-400, PEG-900 and PEG-4000 at 0–3 h, 12–24 h and 1–2 weeks after a satiation meal. Permeability was measured in the mucosal to serosal direction. (B) Simultaneously measured absorptive flux of water in the mucosal to serosal direction in these same preparations. (C) The relative PEG flux to net water flux ratio in these same preparations; if the flux ratio is >1.0, PEG is moving faster than water, and if it is <1.0, PEG is moving at a slower rate than water. See Materials and methods for details. Means + 1 s.e.m. (N=6–9 per treatment). Asterisks indicate significant differences (P<0.05) from the comparable treatments in seawater preparations of Fig. 1. Within a panel, means sharing the same letter are not significantly different from one another (P>0.05).

In control experiments, the elevated serosal osmotic pressure of 580 mosmol kg^{-1} resulted in high, almost identical absorptive water flux in freshwater and seawater gut sacs (Fig. 6A), similar to those measured in the earlier series with seawater preparations (Fig. 4A). These very similar, very high water flux rates under osmotic clamping (Fig. 6A) occurred despite the greater net water flux rates in control freshwater preparations than in control seawater preparations under isosmotic conditions (Fig. 1B, Fig. 2B, Fig. 5A). The effects of 10^{-4} mol l^{-1} $HgCl_2$ in combination with high serosal osmolality were also identical at the two salinities, resulting in a 60% reduction of water flux (Fig. 6A) and a 6- to 8-fold elevation in PEG-4000 permeability (Fig. 6B) in both cases. Therefore, once again, water and PEG flux changed in opposite directions. $HgCl_2$ treatment also reduced, but did not eliminate, absorptive Cl^- flux in both freshwater (1823±77 nmol cm^{-2} h^{-1} N=8 *versus* 4024±438 nmol cm^{-2} h^{-1} N=8) and seawater preparations (1928±138 nmol cm^{-2} h^{-1} N=8 *versus* 4190±204 nmol cm^{-2} h^{-1} N=8) under osmotic clamping.

TAP gut sac experiments

All four experiments with this putative paracellular pathway blocker in the mucosal compartment yielded the same result, so one only is reported in Table 1 Regardless of whether the 20 mmol l^{-1} TAP was added acutely or for 1 h of pre-incubation, or tested at 1–3 or 12–24 h post-feeding, there were no significant effects of the drug on net water flux rates, net Cl^- absorption rates or PEG-4000 permeability.

DISCUSSION

Overview

The present results clearly dissociate the net movement of water from the movement of the paracellular permeability markers PEG-400, PEG-900 and PEG-4000 in the intestine of the killifish. Large changes in absorptive water flux achieved endogenously *via* feeding and fasting (Fig. 1B, Fig. 2B) or exogenously *via* osmotic clamping (Fig. 4) had essentially no effect on PEG permeability, regardless of molecular size. Even when PEG permeability was measured by its flux counter-current to that of water, the values remained unchanged (Fig. 3). A treatment (10^{-3} mol l^{-1} $HgCl_2$) that greatly increased PEG permeability, actually eliminated (Fig. 5) or greatly reduced (Fig. 6) absorptive water flux. Clearly, there is no correlation between PEG movement and net water movement, and no solvent drag effect. We conclude that absorptive water transport must occur by a pathway entirely different from that of PEG, and that is very likely to be *via* a transcellular route involving aquaporins. Although it seems unlikely, we cannot eliminate the possibility that the general

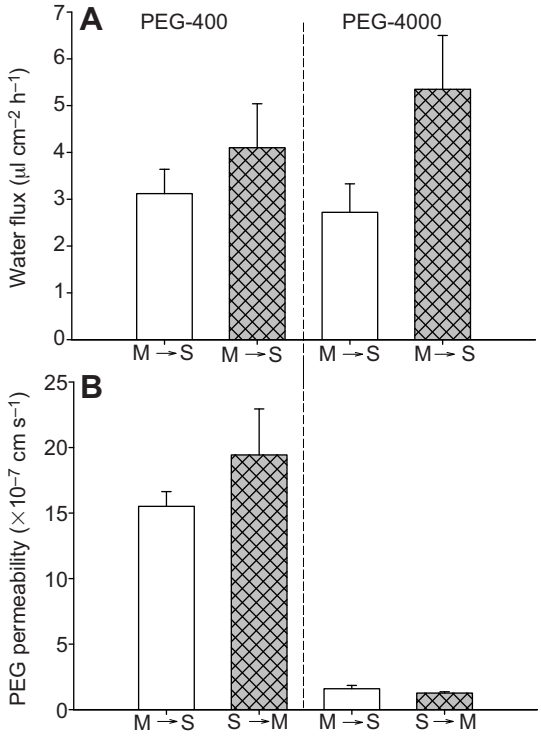

Fig. 3. The influence of the direction of measurement on PEG permeability in intestinal sac preparations from seawater-acclimated killifish at 12–24 h after a satiation meal. (A) Absorptive water flux, measured in the mucosal to serosal (M→S) direction, accompanying the respective PEG permeability measurements in B. (B) Simultaneous PEG-400 permeability (left panel) and PEG-4000 permeability (right panel) measured by tracking PEG radioactivity flux in M→S or S→M directions, i.e. in the same direction or in the opposite direction relative to the net absorptive flow of water from mucosal to serosal compartments (M→S). Means + 1 s.e.m. (N=6–8 per treatment). There were no significant differences with respect to the direction of measurement.

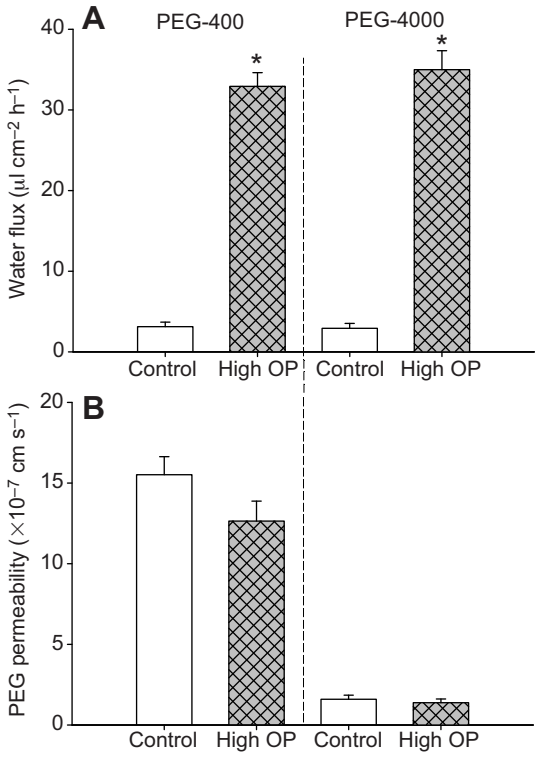

Fig. 4. The influence of raising the serosal osmolality from 303 mosmol kg^{-1} (Control) to 580 mosmol kg^{-1} (high osmotic pressure, High OP), by the addition of 300 mmol l^{-1} mannitol, on (A) the absorptive flux of water and (B) the simultaneously measured permeability to PEG-400 and PEG-4000 in the mucosal to serosal direction in intestinal sac preparations from seawater-acclimated killifish at 12–24 h after a satiation meal. Means + 1 s.e.m. (N=6–8 per treatment). Asterisks indicate significant differences from Control (P<0.05).

lack of change in PEG permeability in all treatments except $HgCl_2$ may reflect the fact that there is a paracellular water pathway entirely separate from the paracellular PEG pathway, hence the finding of no solvent drag. Diffusive unidirectional fluxes in dynamic equilibrium through the paracellular pathway also remain possible, but would not impact on the physiology of the fish.

PEG permeability did tend to be higher in freshwater preparations, and freshwater preparations tended to have higher net water flux (Figs 2 and 5). However, overall this difference in PEG permeability was significant for only one size of PEG molecule (PEG-900), as discussed below (see Fig. 7). Very probably, this reflects different functional properties of the gut in freshwater *versus* seawater killifish with respect to Cl^- uptake, acid–base status and the need for divalent ion barrier functions in seawater fish, rather than indicating a functional relationship between net water flux and PEG permeability. It is noteworthy that under osmotic clamping (control treatments of Fig. 6), the capacity for elevated net water absorption was the same in freshwater and seawater preparations. This supports the view that under isosmotic conditions, the higher net water absorption in freshwater gut sacs reflects functional regulation, rather than a difference in capacity. One other difference was a higher permeability to PEG-4000 in seawater fish that had been fasted for 1–2 weeks (Fig. 1A). In future studies, it would be of interest to examine whether long-term fasting is associated with increased leakiness to other molecules.

TAP had no effect on either PEG permeability or absorptive water flux (Table 1); this observation neither supports nor opposes our conclusions, but this lack of effect is by no means unprecedented. For example, in rabbit and frog gall bladder preparations, where there was strong evidence for paracellular permeability to several small molecules, TAP did not affect net water or Cl^- flux rates, or the permeability to sucrose, a molecule of comparable size to PEG-400 (Moreno, 1975). The author concluded that water was permeating mainly *via* the transcellular route. This is very different from mammalian intestine, where TAP strongly reduces permeability to water and numerous small molecules, suggesting a large paracellular flow of both (Rehman et al., 2003).

PEG permeability as a function of molecular size

The hydrodynamic radii (r, in Å) of PEG molecules are known (Ruddy and Hadzija, 1992) and can be calculated from molecular masses (M) by the relationship:

$$r = 0.29M^{0.454}. \quad (4)$$

Thus the mean hydrodynamic radii of PEG-400, PEG-900 and PEG-4000 are 4.49, 6.36 and 12.52 Å. As PEG permeability was essentially independent of time post-feeding (Fig. 1A, Fig. 2A), mean permeability for all treatments has been plotted against mean hydrodynamic radius for freshwater and seawater preparations in Fig. 7. There appears to be a close to linear negative relationship

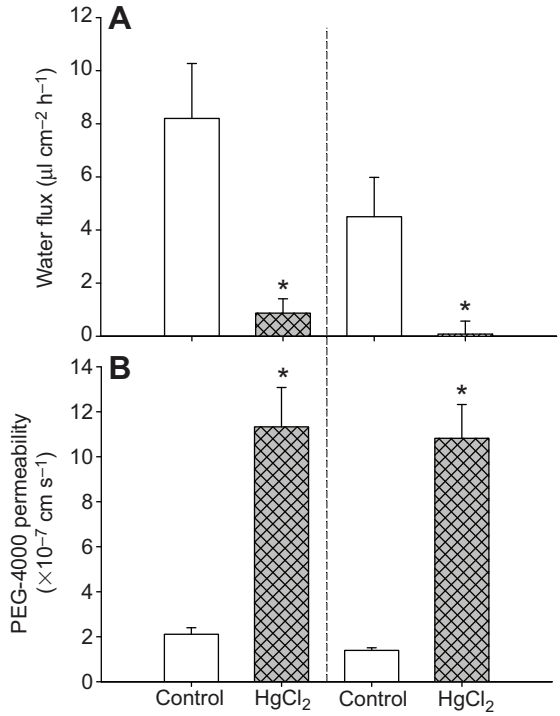

Fig. 5. The influence of 10^{-3} mol l^{-1} $HgCl_2$, applied only to the mucosal surface, on (A) the absorptive flux of water and (B) the simultaneously measured permeability to PEG-4000 in the mucosal to serosal direction in intestinal sac preparations from freshwater-acclimated (left-hand panels) and seawater-acclimated killifish (right-hand panels) at 12–24 h after a satiation meal. Means + 1 s.e.m. (N=6–8 per treatment). Asterisks indicate significant differences from Control (P<0.05). There were no significant differences between freshwater and seawater preparations under the same treatment conditions.

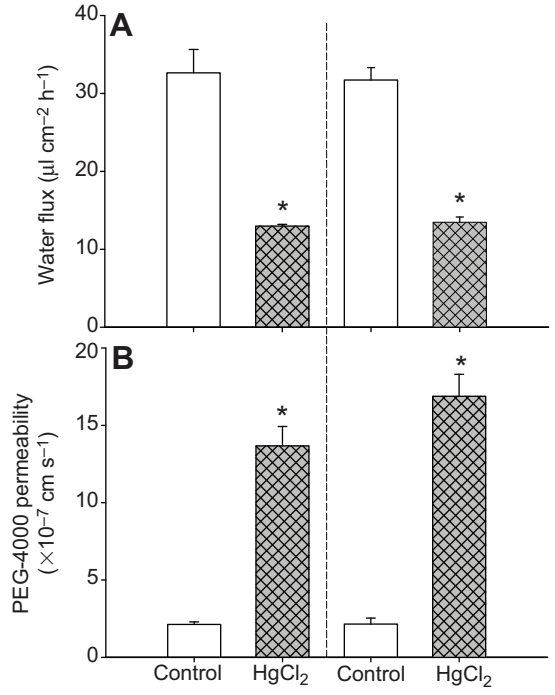

Fig. 6. The influence of 10^{-3} mol l^{-1} $HgCl_2$ applied only to the mucosal surface, in combination with high serosal osmolality (580 mosmol kg^{-1}, achieved by the addition of 300 mmol l^{-1} mannitol), on (A) the absorptive flux of water and (B) the simultaneously measured permeability to PEG-4000 in the mucosal to serosal direction in intestinal sac preparations from freshwater-acclimated (left-hand panels) and seawater-acclimated killifish (right-hand panels) at 12–24 h after a satiation meal. The controls were subjected only to high serosal osmolality. Means + 1 s.e.m. (N=6–8 per treatment). Asterisks indicate significant differences from Control (P<0.05). There were no significant differences between freshwater and seawater preparations under the same treatment conditions.

between PEG permeability and hydrodynamic radius, with the relationship being somewhat elevated (i.e. higher permeability) in the freshwater fish. This difference was significant only at a hydrodynamic radius of 6.36 Å, i.e. for PEG-900, and was not seen in Fig. 2A because of the lower N value in the individual treatments.

These relationships suggest several conclusions. Firstly, by application of the Stokes–Einstein equation, simple free diffusion of the PEG molecules would be inversely proportional to their hydrodynamic radius. Thus, for free diffusion, PEG-400 permeability (4.49 Å) would be 2.79 times greater than PEG-4000 permeability (12.52 Å) and PEG-900 permeability (6.36 Å) would be 1.98 times greater than PEG-4000 permeability. The actual differences are far greater than this (8.00- and 5.57-fold, respectively, in seawater preparations, 8.44- and 7.30-fold, respectively, in freshwater preparations). Thus the paracellular barrier is significant and size selective. Secondly, there appears to be a range of paracellular 'pore' sizes in the intestine of the killifish, and this range is not dissimilar to that in the mammalian small intestine based on comparable PEG permeation studies (Ma et al., 1991; He et al., 1998). Schep and colleagues, using very different methods, reached the same conclusion about pore size in the intestine of the chinook salmon (Schep et al., 1997). Thirdly, there appears to be a greater abundance of 'pores' in the 6.36 Å range in freshwater killifish than in seawater preparations. Finally, the atomic radius of the water molecule itself is only 1.35 Å, smaller than all these pore sizes, so it remains possible that there exists a paracellular pathway for water that would not interact with the paracellular pathways for the various sized PEG molecules. For this last scheme to explain the present

Table 1. The influence of 20 mmol l^{-1} 2,4,6-triaminopyrimidine (TAP) in the mucosal solution on absorptive water flux rates, absorptive Cl^- flux rates and permeability to PEG-4000 in intestinal sac preparations from seawater-acclimated killifish

	Control (N=6)	TAP (N=6)
Water flux rate (µl cm^{-2} h^{-1})	5.32±1.61	4.80±1.33
Cl^- flux rate (nmol cm^{-2} h^{-1})	1412±161	1134±190
PEG-4000 permeability ($\times10^{-7}$ cm s^{-1})	7.33±1.25	9.79±1.72

Data are means ± s.e.m. and were obtained 12–24 h post-feeding. Permeability to PEG-4000 was measured in the mucosal to serosal direction. There were no significant differences (P>0.05).

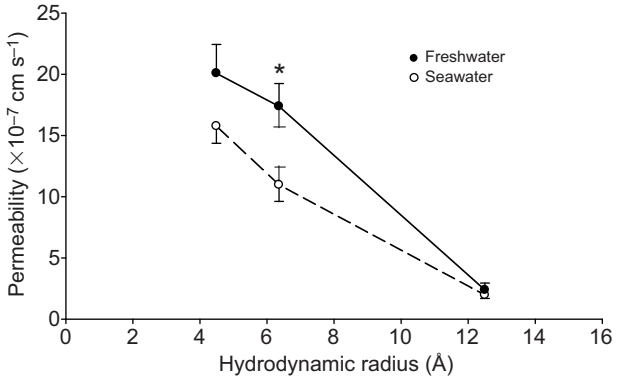

Fig. 7. Relationships between the measured permeability to PEG and the hydrodynamic radius of the PEG molecules in intestinal sac preparations from seawater- and freshwater-acclimated killifish. Mean permeability for all times post-feeding have been plotted against mean hydrodynamic radius (PEG-400, 4.49 Å; PEG-900, 6.36 Å; and PEG-4000, 12.52 Å). Means ± 1 s.e.m. (N=19–26). Asterisk indicates a significant difference (P<0.05) between freshwater and seawater preparations at the same hydrodynamic radius.

data, the larger paracellular PEG pores would have to be low in number relative to the paracellular water channels and would have to selectively exclude water molecules, so that there could be no observed solvent drag effects.

PEG-4000 has been extensively used as a drinking rate marker in fish by many labs, including our own (e.g. Grosell et al., 1999), since its introduction for this purpose (see Shehadeh and Gordon, 1969), on the assumption that it is not absorbed across the fish intestine (e.g. Skadhauge, 1974). However Boge and colleagues (Boge et al., 1988) reported that it was lost at an appreciable rate from an intestinal perfusate in intact trout, and the present study shows that it is absorbed *in vitro* by the killifish intestine, albeit at a low rate. This should be taken into account in future studies of drinking in fish and in studies employing PEG as a 'non-absorbable' marker for water transport in isolated intestinal segments.

A role for aquaporins in intestinal water absorption in fish

The channels by which transcellular water absorption occurs in the intestine of the euryhaline killifish are probably aquaporins. Very recent work (reviewed by Cerda and Finn, 2010; Grosell, 2011a) shows that many different aquaporins are widely expressed in the intestinal tract of euryhaline teleosts, and that AQP1 in particular may play a role in water absorption. Observations of elevated mRNA expression following seawater transfer, elevated AQP1 protein abundance in intestinal tissue following seawater acclimation and, finally, apical as well as basolateral localization of the protein suggest a role in transepithelial water movement (Aoki et al., 2003; Martinez et al., 2005a; Martinez et al., 2005b; Raldua et al., 2008). It has been demonstrated that AQP1 genes from fish confer water permeability in expression systems (MacIver et al., 2009), including AQP1a from *F. heteroclitus* (Tingaud-Sequeira et al., 2009), but despite the above observations, direct evidence for a role for AQP1 in intestinal water absorption has been lacking. Consistent with this view, Cerda and Finn caution that the relative contribution of aquaporin-mediated transcellular flux *versus* paracellular flux is largely unknown (Cerda and Finn, 2010).

In the present experiments, $HgCl_2$ was a highly effective inhibitor of water absorption in killifish intestine (Figs 5 and 6), consistent with the known ability of Hg^{2+} to cause covalent modification of a cysteine within the selectivity filter region of the aquaporin channel pore, resulting in a steric blockade (Savage and Stroud, 2007). The concentration needed to achieve full inhibition was 10^{-3} mol l^{-1}, the same as that required to inhibit fish aquaporins in an oocyte expression system (MacIver et al., 2009). However, 10^{-3} mol l^{-1} $HgCl_2$ had two other notable effects: a 6- to 8-fold elevation of PEG-4000 permeability, and an abolition of absorptive Cl^- flux. The former provides further support for the conclusion that water flux is not associated with the paracellular pathway, and accords with studies on mammalian intestine where $HgCl_2$ similarly increases permeability to paracellular markers (Stirling, 1975; Bohme et al., 1992; Kierbel et al., 2000). Presumably Hg^{2+} interacts with cysteine residues or other SH groups that are crucial in limiting junctional permeability. However, the complete blockade of Cl^- absorption confounds interpretation of the inhibition of net water flux, because the two major mechanisms thought to provide the osmotic linkage for water flux under isosmotic conditions are coupled Na^+ plus Cl^- co-transport, and Cl^-/HCO_3^- exchange (Grosell, 2006; Grosell, 2011a; Grosell, 2011b). The explanation is probably the known potency of Hg^{2+} in inhibiting Na^+,K^+-ATPase and other ATPases (Musch et al., 1990; Lakshmi et al., 1991) that power these mechanisms. Clearly, elimination of net Cl^- transport provides an alternative or additional explanation to blockade of aquaporins for the action of $HgCl_2$ on absorptive water flux.

The treatment with $HgCl_2$ in combination with high serosal osmolality (Fig. 6) was designed to overcome this confounding issue by creating a situation in which net water flux would not be primarily driven by Cl^- transport. Again $HgCl_2$ raised PEG-4000 permeability by 6- to 8-fold, and caused similar inhibition of the now elevated absorptive water flux (by ~60%) and absorptive Cl^- flux (by ~55%). However, as shown by the analysis in Table 2, with high serosal osmolality, the apparent Cl^- concentration in the absorbate was reduced from its normal hypertonic level (~228 mmol l^{-1}) (see also Wood et al., 2010) to values (~128 mmol l^{-1}) below that

Table 2. The influence of high serosal osmolality alone or in the presence of mucosal $HgCl_2$ on the concentration of Cl^- in the absorbate of gut sac preparations from freshwater- or seawater-acclimated killifish

	Freshwater (mmol l^{-1} Cl)	Seawater (mmol l^{-1} Cl)
Incubation saline	152.0	152.0
Control	232.2 ±13.2^x (15)	220.1±16.8^a (13)
High serosal osmolality	122.4±4.6^y (8)	133.2±4.3^b (8)
High serosal osmolality + $HgCl_2$	140.3±4.7^z (8)	142.5±5.0^b (8)

Data are means ± s.e.m. (N) and were obtained 12–24 h after a satiation meal. The Cl^- concentration in the absorbate was estimated by dividing the measured Cl^- absorption rate by the measured net water absorption rate in each preparation. The Cl^- concentration in the incubation saline is shown for comparison.
High serosal osmolality, 580 mosmol kg^{-1}, achieved by the addition of 300 mmol l^{-1} mannitol; mucosal $HgCl_2$ concentration, 10^{-3} mol l^{-1}.
For a given salinity, means sharing the same letter are not significantly different (P>0.05).
There were no significant differences (P<0.05) between freshwater and seawater values under the same treatment conditions.

(152 mmol l^{-1}) of the incubation saline. Clearly, under these conditions, Cl^- absorption was no longer driving water absorption, yet the latter was still strongly inhibited by $HgCl_2$. Additionally, it is noteworthy that the apparent Cl^- concentration of the absorbate rose after $HgCl_2$ treatment (significant in freshwater preparations only, Table 2), suggesting a preferential inhibition of net water flux over net Cl^- flux. Kierbel and colleagues reported a similar strong inhibition of absorptive water flux in response to 0.3×10^{-3} mol l^{-1} $HgCl_2$ in rat and rabbit intestinal preparations subjected to elevated serosal osmolality (Kierbel et al., 2000).

Differences between euryhaline fish and mammals

We are aware of no comparable analysis of the routes of net water flux in the intestine of teleost fish. However, there is a precedent for a completely transcellular flow of water in an electrically 'leaky' epithelium. Using a direct visualization technique, Kovbasnjuk and colleagues reported that water did not flow through the paracellular pathway in an MDCK (renal) cell epithelium, even when osmotic gradients were applied (Kovbasnjuk et al., 1998). However, the situation in the killifish gut appears to be very different from that in the mammalian gut where much of the increased intestinal water absorption accompanying a meal appears to be paracellular, and serves to drive the paracellular absorption of ions and nutrients by convective solvent drag, at minimal metabolic cost (Pappenheimer and Reiss, 1987; Madara and Pappenheimer, 1987). Indeed, a recent review (Bakke et al., 2011) noted that the paracellular uptake of nutrients is generally considered to be negligible in fish. In euryhaline teleosts, the need for precise control of ion and water absorption may be much greater than in mammals because of the intense and variable environmental gradients. Here, intestinal absorption must serve iono- and osmo-regulatory requirements in addition to the need for nutrient absorption. Therefore, this precision may be achieved by running the flux of both water and ions/nutrients (*via* specific channels and transporters) through the transcellular route, thereby more easily controlling the amount of water that follows osmolyte uptake.

One of the benefits of routing all absorptive water flux through the transcellular pathway is that it will avoid unwanted ion uptake by solvent drag. For example, Nadella and colleagues demonstrated that absorption of the essential but toxic ion Cu^{2+} was unrelated to solvent drag, osmotic pressure or changes in transepithelial potential in the gut of the euryhaline rainbow trout (Nadella et al., 2007). Similarly, the uptake of other essential but toxic ions that are at high levels in ingested seawater (Mg^{2+}, SO_4^{2-}) (Grosell, 2006; Grosell, 2011a) can be minimized by ensuring that all ion and water flux is routed through transcellular pathways. Recent findings show that changes in salinity alter mRNA expression of multiple isoforms for claudin 3, 15 and 25b in the intestinal epithelium of euryhaline fish (Clelland et al., 2010; Tipsmark et al., 2010), which suggests that these claudins may be involved in controlling and regulating the paracellular pathway and thus potentially the barrier functions of the epithelium against movement of divalent ions. Of particular interest is that certain isoforms are expressed more robustly in the distal segments where luminal–serosal Mg^{2+}, SO_4^{2-} and HCO_3^- gradients are the steepest (Marshall and Grosell, 2006). It is also noteworthy that aquaporin expression appears to be greatest in the hindgut and rectum of several species (reviewed by Cerda and Finn, 2010). Our killifish intestine preparations excluded part of this area because of its fragility (see Materials and methods), so it is possible that our data underestimate the water absorption capacity of the whole gut. It is also possible, indeed likely, that our data based on almost whole intestinal sacs hide regional differences in transport and permeability along the tract.

The need for precise control of paracellular ion movement, especially in marine fish, may be even more intense in the killifish because of its unusual 'deficit' in freshwater: in contrast to Na^+ uptake, there is no active uptake mechanism for Cl^- at the gills (Patrick et al., 1997; Patrick and Wood, 1999; Wood and Laurent, 2003), so this major and essential anion must be acquired exclusively from the diet. Probably for this reason, intestinal Cl^- (as well as Na^+ and H_2O) uptake rates increase during acclimation to freshwater (Scott et al., 2006), and persist at higher rates than in seawater-acclimated animals (Scott et al., 2008; Wood et al., 2010). The difference becomes more marked at 1–3 and 12–24 h after a meal when Cl^- uptake rate, HCO_3^- secretion rate (to which Cl^- uptake is partially coupled) and water absorption are all significantly greater in freshwater killifish (Wood et al., 2010). The same differences between freshwater and seawater preparations at 12–24 h after the meal, at least for Cl^- and water absorption, were seen in the present study. Notably, the Cl^- concentration of the absorbate increases with time of fasting, as would be predicted if there is a mechanism to control how much water flux follows ion flux through the transcellular pathway. Interestingly, the only other euryhaline teleost that is known to rely on intestinal rather than branchial Cl^- uptake in freshwater is the eel (Kirsch, 1972; Grosell et al., 2000), and here too the concentration of the absorbate was higher in freshwater than in seawater animals (Skadhauge, 1969). Additional experiments (Skadhauge, 1969; Skadhauge, 1974) demonstrated that the intestinal water absorption in the eel was closely linked to, and presumably driven by, the active transport of Na^+ and Cl^-, though the author suggested that this might occur *via* the lateral intercellular spaces (i.e. a paracellular route), in contrast to the current evidence.

Because Cl^- uptake is coupled, at least in part, to HCO_3^- secretion, another consequence of the higher Cl^- and water absorption rates across the intestine in freshwater killifish is a higher pH in the gut lumen, both *in vitro* and *in vivo* (Wood et al., 2010). Paracellular permeability is known to be pH sensitive (e.g. Powell et al., 1981), so the tendency for higher PEG permeability in preparations from freshwater animals, significant for PEG-900 (6.36 Å; Fig. 7), may reflect this acid–base difference. As an HCl-secreting stomach is entirely lacking in *F. heteroclitus* (Babkin and Bowie, 1928), digestion must rely exclusively on mechanical and enzymatic hydrolysis. The products may be different because of the higher pH of the chyme, requiring different pore sizes for the paracellular absorption of large nutrients (e.g. polypeptides) in freshwater *versus* seawater killifish. In addition, teleost aquaporins are known to be more permeable to water at higher pH values (reviewed by Cerda and Finn, 2010), so this may explain the higher water absorption rates in freshwater killifish (Fig. 2B). Clearly, there are many questions that can be pursued using this relatively simple experimental system.

ACKNOWLEDGEMENTS

We thank Linda Diao for excellent technical assistance at McMaster University, and Danielle McDonald for access to equipment in Miami. We also thank the anonymous reviewers for constructive comments, especially the suggestion of the $HgCl_2$ experiment.

FUNDING

This work was supported by a Natural Sciences and Engineering Research Council of Canada (NSERC) Discovery Grant [to C.M.W.] and a National Science Foundation (NSF) grant [IOB 0743903 to M.G.]. C.M.W. is supported by the Canada Research Chair Program.

REFERENCES

Aoki, M., Kaneko, T., Katoh, F., Hasegawa, S., Tsutsui, N. and Aida, K. (2003). Intestinal water absorption through aquaporin 1 expressed in the apical membrane of mucosal epithelial cells in seawater-adapted Japanese eel. *J. Exp. Biol.* **206**, 3495-3505.

Babkin, B. P. and Bowie, D. J. (1928). The digestive system and its function in *Fundulus heteroclitus*. *Biol. Bull.* **54**, 254-277.

Bakke, A. M., Glover, C. and Krogdahl, Å. (2011). Feeding, digestion, and absorption of nutrients. In *The Multifunctional Gut of Fish*, *Fish Physiology*, Vol. 30 (ed. M. Grosell, A. P. Farrell and C. J. Brauner), pp. 57-110. Amsterdam: Academic Press.

Boge, G, Lopez, L. and Peres, G. (1988). An *in vivo* study of the role of pyloric caeca in water absorption in rainbow trout (*Salmo gairdneri*). *Comp. Biochem. Physiol.* **91A**, 9-13.

Böhme, M., Diener, M., Mestres, P. and Rummel, W. (1992). Direct and indirect actions of $HgCl_2$ and methyl mercury chloride on permeability and chloride secretion across the rat colonic mucosa. *Toxicol. Appl. Pharmacol.* **114**, 285-294.

Cerda, J. and Finn, R. N. (2010). Piscine aquaporins: an overview of recent advances. *J. Exp. Zool.* **313A,** 623-650.

Clelland, E. S., Bui, P., Bagherie-Lachidan, M. and Kelly, S. P. (2010). Spatial and salinity-induced alterations in claudin-3 isoform mRNA along the gastrointestinal tract of the pufferfish *Tetraodon nigroviridis*. *Comp. Biochem. Physiol.* **155A**, 154-163.

Grosell, M. (2006). Intestinal anion exchange in marine fish osmoregulation. *J. Exp. Biol.* **209**, 2813-2827.

Grosell, M. (2011a). The role of the gastrointestinal tract in salt and water balance. In *The Multifunctional Gut of Fish*, *Fish Physiology*, Vol. 30 (ed. M. Grosell, A. P. Farrell and C. J. Brauner), pp. 136-164. Amsterdam: Academic Press.

Grosell, M. (2011b). Intestinal anion exchange in marine teleosts is involved in osmoregulation and contributes to the oceanic inorganic carbon cycle. *Acta Physiologica* **202**, 421-434.

Grosell, M. and Jensen, F. B. (1999). NO_2^- uptake and HCO_3^- excretion in the intestine of the European flounder (*Platichthys flesus*). *J. Exp. Biol.* **202**, 2103-2110.

Grosell, M. and Taylor, J. R. (2007). Intestinal anion exchange in teleost water balance. *Comp. Biochem. Physiol.* **148A**, 14-22.

Grosell, M., DeBoeck, G., Johannsson, O. and Wood, C. M. (1999). The effects of silver on intestinal ion and acid-base regulation in the marine teleost fish, *Parophrys vetulus*. *Comp. Biochem. Physiol. C* **124**, 259-270.

Grosell, M., Hogstrand, C., Wood, C. M. and Hansen, J. M. (2000). A nose-to-nose comparison of the physiological effects of exposure to ionic silver versus silver chloride in the European eel (*Anguilla anguilla*) and the rainbow trout (*Oncorhynchus mykiss*). *Aquat. Toxicol.* **48**, 327-343.

Grosell, M., Mager, E. M., Williams, C. and Taylor, J. R. (2009). High rates of HCO_3^- secretion and Cl^- absorption against adverse gradients in the marine teleost intestine; the involvement of an electrogenic anion exchanger and H^+-pump metabolon. *J. Exp. Biol.* **212**, 1684-1696.

He, Y. L., Murby, S., Warhurst, G., Gifford, L., Walker, D., Ayrton, J., Eastmond, R. and Rowland, M. (1998). Species differences in size discrimination in the paracellular pathway reflected by oral availability of poly(ethylene glycol) and D-peptides. *J. Pharmaceutical Sci.* **87**, 626-633.

Hill, A. E. (2008). Fluid transport – a guide for the perplexed. *J. Membr. Biol.* **223**, 1-11.

Kierbel, A., Capurro, C., Pisam, M., Gobin, R., Christensen, B. M., Nielsen, S. and Parisi, M. (2000). Effects of medium hypotonicity on water permeability in the mammalian rectum: ultrastructural and molecular correlates. *Eur. J. Physiol.* **440**, 609-618.

Kirsch, R. (1972). The kinetics of peripheral exchanges of water and electrolytes in the silver eel (*Anguilla anguilla* L.) in fresh water and sea water. *J. Exp. Biol.* **57**, 489-512.

Kovbasnjuk, O., Leader, J. P., Weinstein, A. M. and Spring, K. R. (1998). Water does not flow across the tight junctions of MDCK cell epithelium. *Proc. Natl. Acad. Sci. USA* **95**, 6526-6530.

Lakshmi, R., Kundu, R., Thomas, E. and Mansuri, A. P. (1991). Mercuric chloride-induced inhibition of different ATPases in the intestine of mudskipper, *Boleophthalmus dentatus*. *Ecotoxicol. Environ. Saf.* **21**, 18-24.

Ma, T. Y., Hollander, D., Erickson, R. A., Truong, H. and Krugliak, P. (1991). Is the small intestinal epithelium truly 'tight' to inulin permeation? *Am. J. Physiol. Gastrointest. Liver Physiol.* **260**, G669-G676.

MacIver, B., Cutler, C. P., Yin, J., Hill, M. G., Zeidel, M. L. and Hill, W. G. (2009). Expression and functional characterization of four aquaporin water channels from the European eel (*Anguilla anguilla*). *J. Exp. Biol.* **212**, 2856-2863.

Madara, J. L. and Pappenheimer, J. R. (1987). Structural basis for physiological regulation of paracellular pathways in intestinal epithelia. *J. Membr. Biol.* **100**, 149-164.

Marshall, W. S. and Grosell, M. (2006). Ion transport, osmoregulation and acid-base balance. *Physiology of Fishes*, 3rd Edn (ed. D. Evans and J. B. Claiborne). Boca Raton, FL: CRC Press.

Martinez, A.-S., Cutler, C. P., Wilson, G. D., Phillips, C., Hazon, N. and Cramb, G. (2005a). Cloning and expression of three aquaporin homologues from the European eel (*Anguilla anguilla*): effects of seawater acclimation and cortisol treatment on renal expression. *Biol. Cell.* **97**, 615-627.

Martinez, A.-S., Cutler, C. P., Wilson, G. D., Phillips, C., Hazon, N. and Cramb, G. (2005b). Regulation of expression of two aquaporin homologs in the intestine of the European eel: effects of seawater acclimation and cortisol treatment. *Am. J. Physiol. Regul. Integr. Comp. Physiol.* **288**, R1733-R1743.

Moreno, J. H. (1975). Routes of non-electrolyte permeability in gallbladder. Effects of 2,4,6-triaminopyrimidinium (TAP). *J. Gen. Physiol.* **66**, 117-128.

Musch, M. W., Chauncey, B., Schmid, E. C., Kinne, R. K. H. and Goldstein, L. (1990). Mechanisms of mercurial and arsenical inhibition of tyrosine absorption in intestine of the winter flounder, *Pseudopleuronectes americanus*. *Toxicol. Appl. Pharmacol.* **104**, 59-66.

Nadella, S. R., Grosell, M. and Wood, C. M. (2007). Mechanisms of dietary Cu uptake in freshwater rainbow trout: evidence for Na-assisted Cu transport and a specific metal carrier in the intestine. *J. Comp. Physiol. B.* **177**, 433-446.

Pappenheimer, J. R. and Reiss, K. Z. (1987). Contribution of solvent drag through intercellular junctions to absorption of nutrients by the small intestine of the rat. *J. Membr. Biol.* **100**, 123-136.

Patrick, M. L. and Wood, C. M. (1999). Ion and acid-base regulation in the freshwater mummichog (*Fundulus heteroclitus*): a departure from the standard model for freshwater teleosts. *Comp. Biochem. Physiol.* **122A**, 445-456.

Patrick, M. L., Pärt, P., Marshall, W. S. and Wood, C. M. (1997). Characterization of ion and acid-base transport in the fresh water adapted mummichog (*Fundulus heteroclitus*). *J. Exp. Zool.* **279**, 208-219.

Powell, D. W. (1981). Barrier function of epithelia. *Am. J. Physiol. Gastrointest. Liver Physiol.* **241,** G275-G288.

Raldua, D., Otero, D., Fabra, M. and Cerda, J. (2008). Differential localization and regulation of two aquaporin-1 homologs in the intestinal epithelia of the marine teleost *Sparus aurata*. *Am. J. Physiol. Regul. Integr. Comp. Physiol.* **294,** R993-R1003.

Rehman, K. U., Wingertzahn, M. A., Teichberg, S., Harper, R. G. and Wapnir, R. A. (2003). Gum Arabic (GA) modifies paracellular water and electrolyte transport in the small intestine. *Dig. Dis. Sci.* **48**, 755-760.

Ruddy, S. B. and Hadzija, B. W. (1992). Iontophoric permeability of polyethylene glycols through hairless rat skin: application of hydrodynamic theory for hindered transport through liquid-filled pores. *Drug Des. Discov.* **8**, 207-224.

Savage, D. F. and Stroud, R. M. (2007). Structural basis of aquaporin inhibition by mercury. *J. Mol. Biol.* **368**, 607-617.

Schep, L. J., Tucker, I. G., Young, G. and Butt, A. G. (1997). Regional permeability differences between the proximal and distal portions of the isolated salmonid posterior intestine. *J. Comp. Physiol. B* **167**, 370-377.

Scott, G. R., Schulte, P. M. and Wood, C. M. (2006). Plasticity of osmoregulatory function in the killifish intestine: drinking rates, water transport, and gene expression after freshwater transfer. *J. Exp. Biol.* **209**, 4040-4050.

Scott, G. R., Baker, D. W., Schulte, P. M. and Wood, C. M. (2008). Physiological and molecular mechanisms of osmoregulatory plasticity in killifish after seawater transfer. *J. Exp. Biol.* **211**, 2450-2459.

Shehadeh, Z. H. and Gordon, M. S. (1969). The role of the intestine in salinity adaptation of the rainbow trout, *Salmo gairdneri*. *Comp. Biochem. Physiol.* **30**, 397-418.

Skadhauge, E. (1969). The mechanism of salt and water absorption in the intestine of the eel (*Anguilla anguilla*) adapted to waters of various salinities. *J. Physiol.* **204**, 135-158.

Skadhauge, E. (1974). Coupling of transmural flows of NaCl and water in the intestine of eel (*Anguilla anguilla*). *J. Exp. Biol.* **60**, 535-546.

Stirling, C. E. (1975). Mercurial perturbation of brush border membrane permeability in rabbit ileum. *J. Membr. Biol.* **23**, 33-56.

Tingaud-Sequeira, A., Zapater, C., Chauvigne, F., Otero, D. and Cerda, J. (2009). Adaptive plasticity of killifish (*Fundulus heteroclitus*) embryos: dehydration-stimulated development and differential aquaporin-3 expression. *Am. J. Physiol. Regul. Integr. Comp. Physiol.* **296**, R1041-R1052.

Tipsmark, C. K., Sorensen, K. J., Hulgard, K. and Madsen, S. S. (2010). Claudin-15 and -25b expression in the intestinal tract of Atlantic salmon in response to seawater acclimation, smoltification and hormone treatment. *Comp. Biochem. Physiol.* **155A**, 361-370.

Watson, C. J., Rowland, M. and Warhurst, G. (2001). Functional modeling of tight junctions in intestinal cell monolayers using polyethylene glycol oligomers. *Am. J. Physiol. Heart Circ. Physiol.* **281**, C388-C397**.**

Whittembury, G., Verde de Martinez, C., Linares, H. and Paz-Aliaga, A. (1980). Solvent drag of large solutes indicates paracellular water flow in leaky epithelia. *Proc. R. Soc. Lond. B* **211**, 63-81.

Wilson, R. W. and Grosell, M. (2003). Intestinal bicarbonate secretion in marine teleost fish-source of bicarbonate, pH sensitivity, and consequence for whole animal acid-base and divalent cation homeostasis. *Biochim. Biophys. Acta* **1618**, 163-193.

Wilson, R. W., Wilson, J. M. and Grosell, M. (2002). Intestinal bicarbonate secretion by marine teleost fish – why and how? *Biochim. Biophys. Acta* **1566**, 182-193.

Wolf, K. (1963). Physiological salines for fresh-water teleosts. *Prog. Fish Cult.* **25**, 135-140.

Wood, C. M. and Grosell, M. (2008). A critical analysis of transepithelial potential in intact killifish (*Fundulus heteroclitus*) subjected to acute and chronic changes in salinity. *J. Comp. Physiol. B* **178**, 713-727.

Wood, C. M. and Laurent, P. (2003). Na^+ versus Cl^- transport in the intact killifish after rapid salinity transfer. *Biochim. Biophys. Acta* **1618**, 106-119.

Wood, C. M., Bucking, C. and Grosell, M. (2010). Acid-base responses to feeding and intestinal Cl^- uptake in freshwater- and seawater-acclimated killifish, *Fundulus heteroclitus*, an agastric euryhaline teleost. *J. Exp. Biol.* **213**, 2681-2692.